

## ENERGY-ABSORPTION BUILDUP FACTORS AND SPECIFIC ABSORBED FRACTIONS OF ENERGY FOR BIOACTIVE GLASSES

M. I. SAYYED<sup>a,\*</sup>, H. C. MANJUNATHA<sup>b</sup>, D. K. GAIKWAD<sup>c</sup>,  
S. S. OBAID<sup>c</sup>, M. H. M. ZAID<sup>d,e</sup>, K. A. MATORI<sup>d,e</sup>

<sup>a</sup>*Department of Physics, Faculty of Science, University of Tabuk, Tabuk, KSA*

<sup>b</sup>*Department of Physics, Government College for Women, Kolar 563101, Karnataka, India*

<sup>c</sup>*Department of Physics, Dr. Babasaheb Ambedkar Marathwada University, Aurnagabad, India:431004.*

<sup>d</sup>*Department of Physics, Faculty of Science, Universiti Putra Malaysia, 43400 UPM Serdang, Selangor, Malaysia.*

<sup>e</sup>*Materials Synthesis and Characterization Laboratory, Institute of Advanced Technology, Universiti Putra Malaysia, 43400 UPM Serdang, Selangor, Malaysia.*

In the present work, effective atomic numbers  $Z_{\text{eff}}$ , energy-absorption buildup factors EABF and specific absorbed fractions of energy ( $\Phi$ ) for different bioactive glasses have been calculated in the present work. Geometric-Progression (G-P) fitting method was used for computation of EABF. The computed EABF is used to estimate the values of  $\Phi$ . It is shown that the EABF and  $\Phi$  are dependent on  $Z_{\text{eff}}$  and mean free path. In addition, EABF and  $\Phi$  were the largest for S4 and S7. The results in this work could be useful in choosing a suitable type of these glasses which in turn are able to resist possible radiation damages at human body and to determine the thickness and shape of the bioactive glasses needed.

(Received March 8, 2018; Accepted August 3, 2018)

*Keywords:* Bioactive glasses, Effective atomic number, Absorption, Ionizing radiations

### 1. Introduction

Bioactive glasses (BG) are perfect candidates for the fabrication of orthopaedic implants. In fact, it is widely known that bioactive glasses, particularly silicate ones, can interact with the host bone tissue after implantation, creating a stable interface which is a preliminary requirement for the prosthesis' fixation. Recently, BG have found wide applications in biomedicine, mainly for replacement or repair of damaged bone and teeth due to disease or trauma. The first bioactive glass (45S5 Bioglass, which contains 46.1% of  $\text{SiO}_2$ , with  $\text{Na}_2\text{O}$ ,  $\text{CaO}$  and  $\text{P}_2\text{O}_5$  as remaining constituents) proposed by Prof. Hench at the end of the 1960s. The 45S5 Bioglass, which is the main representative of this group, has been approved by the US FDA and it has been applied in clinical practice for the treatment of periodontal diseases, for middle-ear surgery and for orthopaedic implants.

In recent times, research interest BG has been encouraged by their various unique properties like (1) a fast rate of surface reaction leading to their direct attachment to bone through a chemical bond; (2) their superior controllability over an extensive range of chemical properties and rate of bonding with tissues and (3) the simplicity of compositional design with properties specific to special clinical applications (Hench, 2006; Salman et al., 2012; Huebsch and Moone, 2009; Seuss et al., 2016).

Ionizing radiations are any types of photon radiation (X-rays and Gamma rays) or particle radiation (electron, proton, neutron and alpha particles) with enough energy to ionize atoms or molecules. It is now fairly well established that exposure to ionizing radiation causes damage to

---

\*Corresponding author: mabualssayed@ut.edu.sa

living cells and organism. The degree of damaged caused by ionizing radiation depends on many factors, of which three are particularly important (1)the types of radiation (alpha, beta, gamma rays..etc), (2) the degree of the exposure (the time that the cell is exposed to the radiation), and (3) the location of the radiation-that is, whether it is inside or outside the body(Chanthima, and Kaewkhao).

X-rays and Gamma rays are generally used for diagnostic in medicine, radiation therapy, gamma knife radio surgery, and for treatment of tumors and other diseases. Accordingly, various organs, tissues and bioactive glasses are exposed to these deleterious radiations. When a small part of the human body is supersede by bioactive material, it is necessary to understand how these materials can be influenced by exposing with the ionized radiations (Hosseinimehr, 2007).Therefore it is important to have the information about the interaction between these radiations with the bioactive glasses. Since when photons come in the human body, they degrade their energy and build up inside the body, giving rise to secondary radiation. This secondary radiation can be calculated by the buildup factors (Sidhu et al., 2000).

There are two types of buildup factor: (1) the energy absorption buildup factor (EABF)and (2) the exposure buildup factor (EBF). These two factors are usually calculated by the widely used method of G-P least square fitting (Harima et al., 1986; Sayyed and Elhouichet, 2017).The specific absorbed fraction of energy ( $\Phi$ ) for bioactive glasses may be calculated from the values of buildup factors. It is defined as the ratio of the energy absorbed by the target to the energy emitted by the source (Manjunatha and Rudraswamy, 2011).

The main aim of this work is to study the gamma-ray interactions with bioactive glasses by calculating the effective atomic number ( $Z_{\text{eff}}$ ), the energy absorption buildup factor (EABF) and the specific absorbed fraction of energy ( $\Phi$ ) in the photons energy range of 0.015 MeV to 15 MeV. The effect of some parameters such as photon energy and penetration depth on EABF and  $\Phi$  has been investigated. With appropriate knowledge of buildup of photons in bioactive glasses, absorbed dose in human body can be carefully controlled. The results of this work may be useful in choosing a suitable type of these glasses which in turn are able to resist possible radiation damages at human body and to determine the thickness and shape of the bioactive glasses needed. The chemical composition of bioactive glasses investigated in this work is presented in Table 1.

Table 1. Compositions of the investigated bioactive glasses in weight fraction.

Bioactive glass	B	O	Na	Mg	Si	P	K	Ca	Zn
S1	0	0.3947	0.1877	0	0.2061	0.0113	0	0.2001	0
S2	0	0.3679	0.1395	0	0.1744	0.0209	0	0.1351	0.1623
S3	0	0.3957	0.1729	0	0.1991	0.0249	0	0.1672	0.0401
S4	0	0.4292	0.1957	0.1392	0.2312	0.0047	0	0	0
S5	0	0.445	0	0	0.280	0.017	0	0.257	0
S6	0	0.3840	0.1669	0	0.1987	0.0104	0	0.1772	0.0627
S7	0	0.4163	0.1957	0.0696	0.2312	0.0047	0	0.0825	0

## 2. Methodology

The computational work of the specific absorbed fraction of energy has been performed in three parts as follows:

### 2.1 Calculation of the effective atomic number $Z_{\text{eff}}$

The mass attenuation coefficient ( $\mu/\rho$ ) is the basic tool used to derive the effective atomic number. In case of mixture of elements, the mass attenuation coefficient can be evaluated using the mixture rule given by the relation (Singh and Badiger, 2015; Sayyed, 2016a).

$$\mu/\rho = \sum_i w_i(\mu/\rho)_i \quad (1)$$

where  $w_i$  and  $(\mu/\rho)_i$  are the weight fraction and the mass attenuation coefficient of the  $i$ th element respectively. For the selected bioactive glasses systems the  $(\mu/\rho)_i$  have been calculated by the WinXcom program (Gerward et al., 2004). For a chemical compound the quantity  $w_i$  is given by  $w_i = a_i A_i / \sum_j^n a_j A_j$ , where  $a_i$  is the number of formula units in the sample and  $A_i$  is the atomic weight of the  $i$ th element.

The total atomic cross section of the samples ( $\sigma_t$ ) can be determined from the  $\mu/\rho$  values using the following equation:

$$\sigma_t = \frac{(\mu/\rho)A_t}{N_A} \quad (2)$$

where  $A_t$  and  $N_A$  represent the molecular weight and Avogadro's number respectively. The effective atomic cross-section ( $\sigma_a$ ) can be calculated using the following equation:

$$\sigma_a = \frac{1}{N_A} \sum f_i A_i (\mu/\rho)_i \quad (3)$$

where  $f_i$  denotes the fractional abundance of element  $i$  with respect to number of atoms.

The total electronic cross-section ( $\sigma_e$ ) is calculated using the following equation:

$$\sigma_e = \frac{1}{N_A} \sum \frac{f_i A_i}{Z_i} (\mu/\rho)_i = \frac{\sigma_a}{Z_{\text{eff}}} \quad (4)$$

where  $Z_i$  is the atomic number of the  $i$ th element. Finally, the  $Z_{\text{eff}}$  of the sample is given by the relation (Manohara and Hanagodimath, 2007):

$$Z_{\text{eff}} = \frac{\sigma_a}{\sigma_e} \quad (5)$$

## 2.2 Calculation of buildup factor

In order to calculate the buildup factor, firstly we have calculated the equivalent atomic number ( $Z_{\text{eq}}$ ) for each sample which illustrates the properties of the composite material in terms of equivalent element and can be expressed as follows (Harmia et al, 1993):

$$Z_{\text{eq}} = \frac{Z_1(\log R_2 - \log R) + Z_2(\log R - \log R_1)}{(\log R_2 - \log R_1)} \quad (6)$$

where  $Z_1$  and  $Z_2$  represent the atomic numbers of elements corresponding to the ratios  $R_1$  and  $R_2$  respectively,  $R$  is the ratio of Compton partial mass attenuation coefficients ( $\mu_{\text{compton}}$ ) to the total mass attenuation coefficients ( $\mu_{\text{total}}$ ) for the chosen bioactive glass at specific energy value. The change in the equivalent atomic numbers ( $Z_{\text{eq}}$ ) with photon energy for the bioactive glasses is shown in Table 2. The G-P fitting parameters ( $b$ ,  $c$ ,  $a$ ,  $X_k$  and  $d$ ) are evaluated in a similar manner of logarithmic interpolation procedure for  $Z_{\text{eq}}$  (Sayed and Elhouichet, 2017; Dong et al., 2018). The energy absorption G-P fitting parameters for S1 are shown in Table 3 as an example.

Table 2. Equivalent atomic number for different bioactive glasses

Energy (MeV)	S1	S2	S3	S4	S5	S6	S7
0.015	13.667	17.394	14.611	11.092	14.365	15.309	12.301
0.02	13.792	17.857	14.811	11.128	14.501	15.545	12.389
0.03	13.915	18.062	15.029	11.169	14.635	15.802	12.484
0.04	14.003	18.277	15.181	11.195	14.727	15.965	12.544
0.05	14.068	18.436	15.284	11.211	14.784	16.084	12.584
0.06	14.113	18.560	15.362	11.217	14.836	16.181	12.620
0.08	14.174	18.735	15.472	11.234	14.902	16.306	12.665
0.1	14.203	18.845	15.541	11.246	14.939	16.383	12.702
0.15	14.271	18.999	15.659	11.224	15.005	16.504	12.758
0.2	14.307	19.172	15.833	11.169	15.090	16.666	12.714
0.3	14.459	19.335	15.669	10.054	15.254	16.865	13.307
0.4	14.411	19.354	15.884	11.101	15.130	16.852	12.746
0.5	14.374	19.401	15.903	11.275	15.176	16.854	12.682
0.6	14.031	19.470	15.821	11.988	15.343	16.863	12.902
0.8	14.031	19.419	16.041	11.995	15.281	16.859	12.900
1	14.022	19.343	16.048	11.996	14.866	17.301	12.924
1.5	12.653	16.729	14.052	10.673	13.983	14.334	11.319
2	12.380	15.484	13.055	10.824	13.098	13.608	11.426
3	12.298	14.776	12.812	10.595	13.008	13.337	11.283
4	12.292	14.716	12.748	10.530	12.942	13.262	11.236
5	12.270	14.660	12.738	10.550	12.869	13.211	11.273
6	12.285	14.608	12.725	10.551	12.853	13.164	11.292
8	12.292	14.580	12.712	10.544	12.874	13.167	11.283
10	12.263	14.580	12.704	10.569	12.879	13.171	11.251
15	12.278	14.552	12.696	10.542	12.857	13.140	11.267

Table 3. G-P energy absorption (EABF) buildup factor coefficients for S1

Energy (MeV)	EBF				
	<b>b</b>	<b>c</b>	<b>a</b>	<b>X<sub>k</sub></b>	<b>d</b>
0.015	1.024	0.398	0.206	12.122	-0.108
0.02	1.055	0.410	0.192	16.955	-0.112
0.03	1.184	0.397	0.214	14.372	-0.117
0.04	1.401	0.455	0.189	14.610	-0.105
0.05	1.670	0.598	0.122	16.737	-0.062
0.06	2.155	0.596	0.142	13.576	-0.079
0.08	3.007	0.803	0.070	13.906	-0.052
0.1	3.658	1.006	0.015	13.753	-0.029
0.15	4.017	1.322	-0.055	15.622	0.007
0.2	3.688	1.476	-0.081	14.929	0.021
0.3	3.120	1.557	-0.096	14.314	0.026
0.4	2.791	1.553	-0.097	14.847	0.028
0.5	2.578	1.527	-0.094	15.034	0.028
0.6	2.433	1.496	-0.091	15.008	0.028
0.8	2.242	1.424	-0.081	15.084	0.027

Energy (MeV)	EBF				
	<b>b</b>	<b>c</b>	<b>a</b>	<b>X<sub>k</sub></b>	<b>d</b>
1	2.124	1.358	-0.071	14.981	0.024
1.5	1.940	1.246	-0.052	14.649	0.020
2	1.834	1.163	-0.035	14.603	0.012
3	1.695	1.060	-0.012	13.549	0.000
4	1.606	0.992	0.006	13.943	-0.009
5	1.545	0.928	0.027	13.339	-0.026
6	1.471	0.931	0.025	15.311	-0.029
8	1.378	0.910	0.032	12.618	-0.024
10	1.309	0.914	0.031	14.497	-0.027
15	1.230	0.841	0.060	14.171	-0.054

The calculated G-P fitting parameters for bioactive glasses then utilized to calculate the gamma ray energy absorption buildup factors (EABF) in the energy range 0.015 MeV-15 MeV up to 40 mean free path (mfp) penetration depths using the equations (Sayyed et.al., 2018):

$$B(E, x) = \begin{cases} 1 + \frac{b-1}{K-1}(K^x - 1) & , K \neq 1 \\ 1 + (b-1)x & , K = 1 \end{cases} \quad (7)$$

where,

$$K(E, x) = cx^a + d \frac{\tanh(x/X_k - 2) - \tanh(-2)}{1 - \tanh(-2)} \quad , x \leq 40 \text{ mfp} \quad (8)$$

where  $x$  is the penetration depth in mfp,  $E$  is the energy of the incident photon,  $K$  is the photon dose multiplicative factor and represent the spectrum shape change, and  $(b, c, a, X_k, d)$  are the calculated G-P fitting parameters in the previous step;

where  $x$  is the source-detector distance for the medium in terms of mfp,  $E$  is the energy of the incident photon, and  $K(E, x)$  is the dose multiplicative factor.

### 2.3 Calculation of specific absorbed fraction of energy ( $\Phi$ )

The calculated EABF values then used to evaluate  $\Phi$  which intern helps for accurate dose calculation in bioactive glasses using the following formula (Manjunatha and Rudraswamy, 2012)

$$\Phi(x) = \frac{\mu_{en} \exp(\mu x) B_{en}}{4\pi x^2 \rho} \quad (9)$$

where  $\mu_{en}$  is linear absorption coefficient of photons at certain energy,  $\mu$  is linear attenuation coefficient of photons at certain energy,  $B_{en}$  is the EABF values and  $\rho$  is density of the medium.

## 3. Results and discussion

The effective atomic numbers ( $Z_{eff}$ ) for the bioactive glasses for photon energy 0.015–15 MeV are shown in Fig. 1. From Fig. 1 it is clear that in the low energy region ( $E < 0.1$  MeV) the  $Z_{eff}$  decrease with increase the energy whereas in the intermediate energy region the  $Z_{eff}$  was found independent upon energy and again increasing in high-energy region. The variation in  $Z_{eff}$  values with photon energy can be explained by partial photon interaction processes, viz. photoelectric absorption, Compton scattering and pair production) appearing at lower, intermediate and higher energy regions respectively (Lakshminarayana et.al., 2018). In addition, it can be seen that the maximum  $Z_{eff}$  was for S2 and this may be for the reason that it contains relatively high Z-element; Ca ( $Z=20$ , weight fraction=0.1351) and Zn ( $Z=30$ , weight fraction=0.1623).

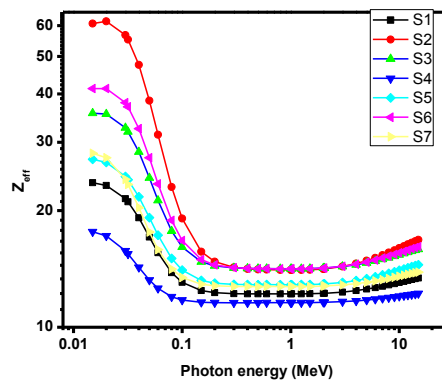


Fig. 1 Effective atomic number  $Z_{eff}$  of the selected bioactive glasses with photon energy from 0.015–15 MeV.

Variation of absorption buildup factors, EABF for the bioactive glasses against photon energy (0.015-15 MeV) is shown in Fig. 2(a-d). It can be seen that the EABF increase up to maximum value then again decreases. The variation for EABF with incident photon energy can be explained by photon interaction process similar to above effective atomic number. The EABF for the bioactive glasses are minimum in low-energy due to dominance of photoelectric effect. With the increment in incident photon energy, EABF increase due to multiple scattering as Compton scattering dominates. In the high-energy region, the pair production takes over the Compton scattering process results in reduces the EABF to a minimum value (El-Mallawany et.al., 2017).

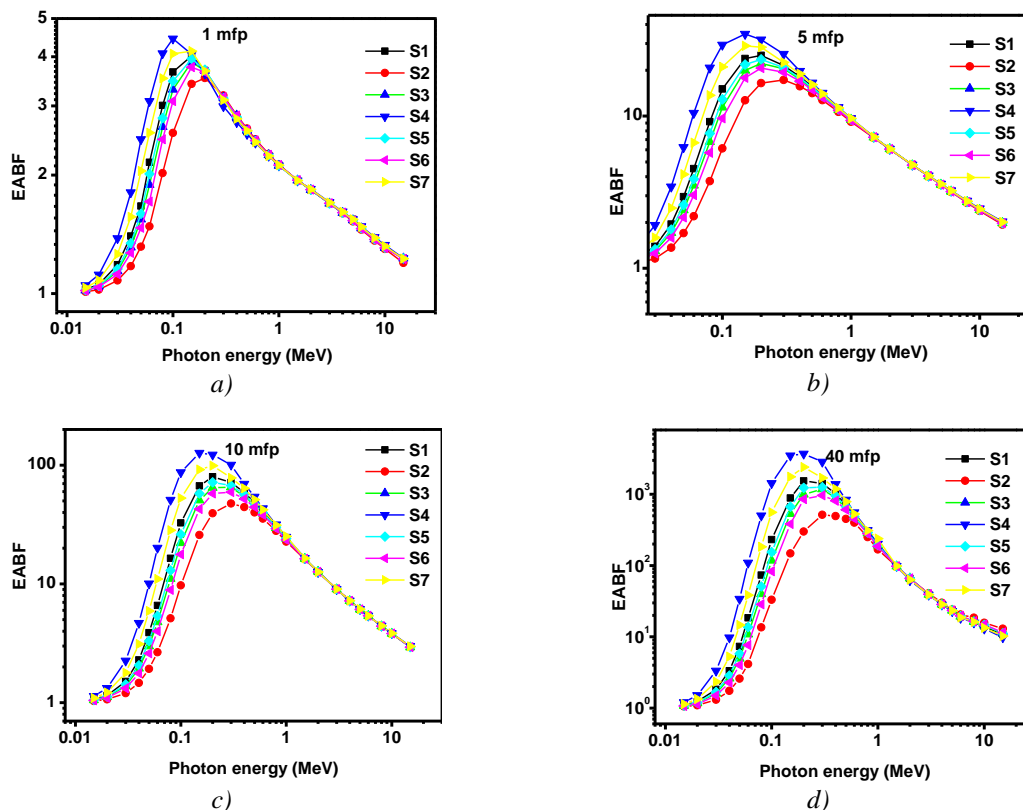


Fig. 2. Variation of energy absorption buildup factors (EABF) the selected bioactive glasses with photon energy at a) 1mfp; b) 5 mfp; c)10 mfp and d) 40 mfp.

It is also seen that the low  $Z_{eff}$  bioactive glass (i.e. S4) dominates the maximum values of EABF while the high  $Z_{eff}$  bioactive glass (i.e.S2) dominates the minimum values of EABF. In

addition, one can observed that the maximum values of EABF shift to higher energies for high  $Z_{\text{eff}}$  glass. For example, the maximum value of EABF occurs at 0.15 MeV for S4 (lowest  $Z_{\text{eff}}$ ), while the maximum value of EABF occurs at 0.3 MeV for S2 (highest  $Z_{\text{eff}}$ ).

The variation of specific fraction of absorbed energy ( $\Phi$ ) with incident photon for all bioactive glasses at different distances ( $r = 0.01, 0.1$  and  $1\text{mm}$ ) for penetration depths 1, 10, 20 and 40 mfp are shown in Figs. (3-5). The specific fraction of absorbed energy ( $\Phi$ ) values decrease with increase in energy up to few keV (80keV) and afterwards increases up to the  $E_{\text{pe}}$  and then decreases. Here  $E_{\text{pe}}$  is the energy value at which the photo electric interaction coefficients matches with Compton interaction coefficients for a given value of effective atomic number ( $Z_{\text{eff}}$ ) (Manjunatha and Rudraswamy, 2011). The variation of  $\Phi$  with energy is due to dominance of photoelectric absorption in the lower end and dominance of pair production in the higher photon energy region.

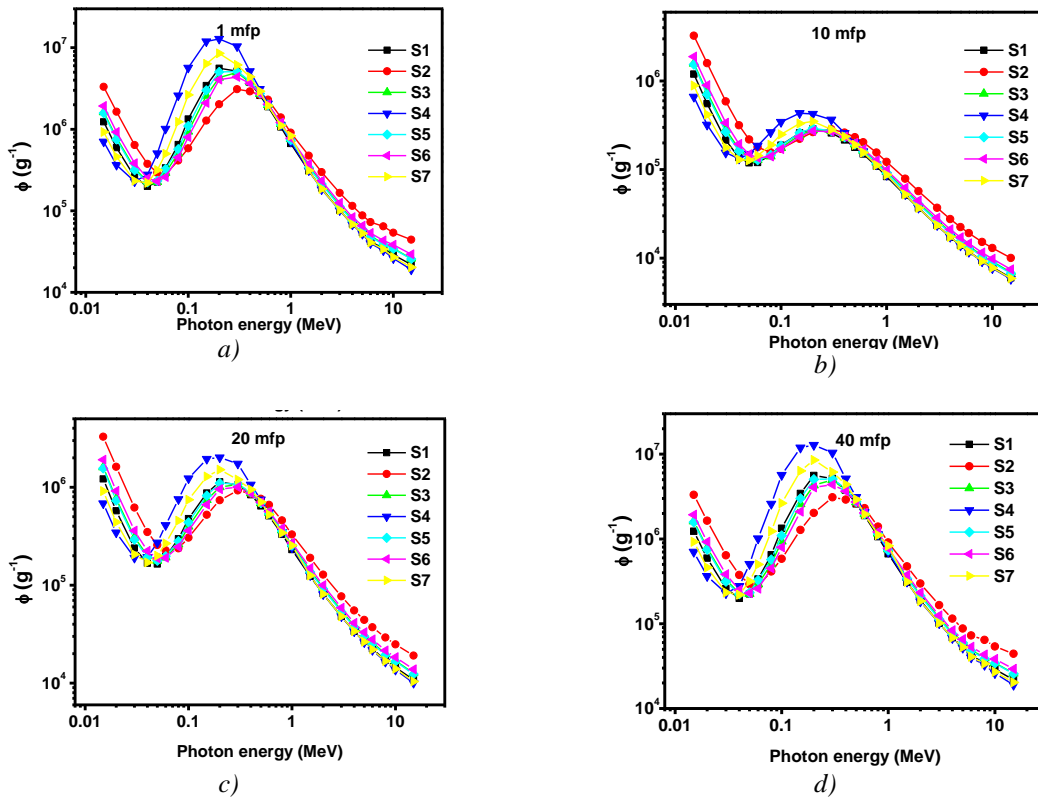


Fig. 3a. The variation of specific fraction of absorbed energy ( $\Phi$ ) with incident photon for all bioactive glasses at  $r = 0.01$  mm and a) 1 mfp; b) 10 mfp; c) 20 mfp; d) 40 mfp.

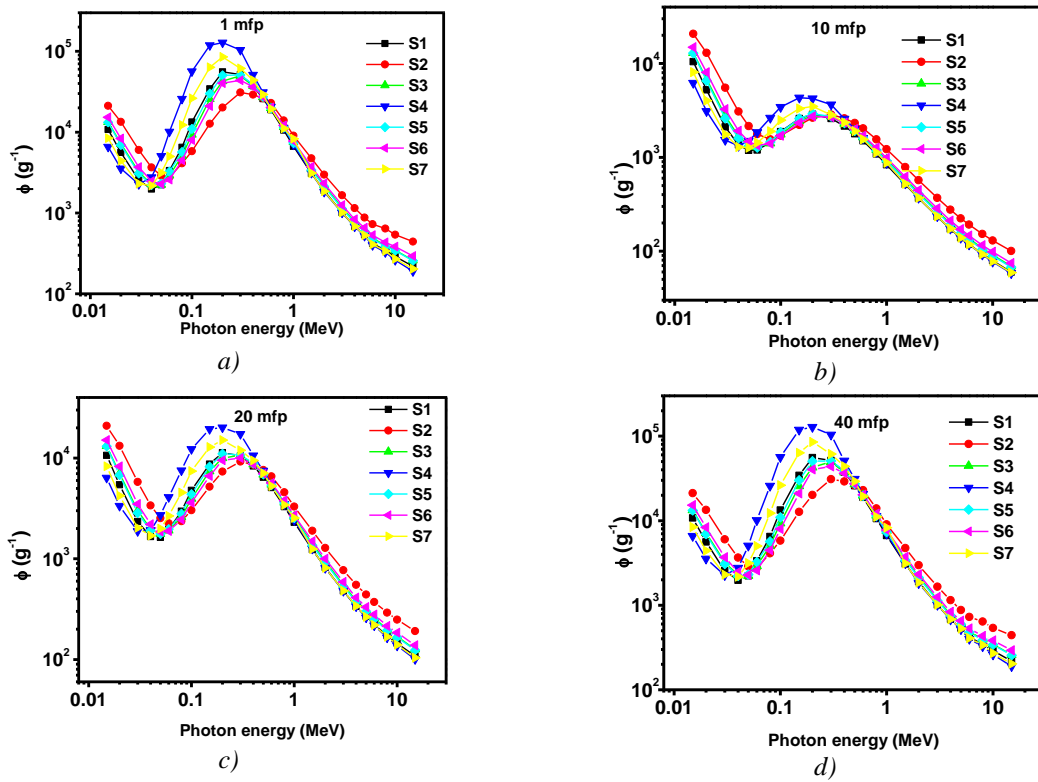


Fig. 4. The variation of specific fraction of absorbed energy ( $\Phi$ ) with incident photon for all bioactive glasses at  $r = 0.1$  mm at a) 1 mfp; b) 10 mfp; c) 20 mfp; d) 40 mfp.

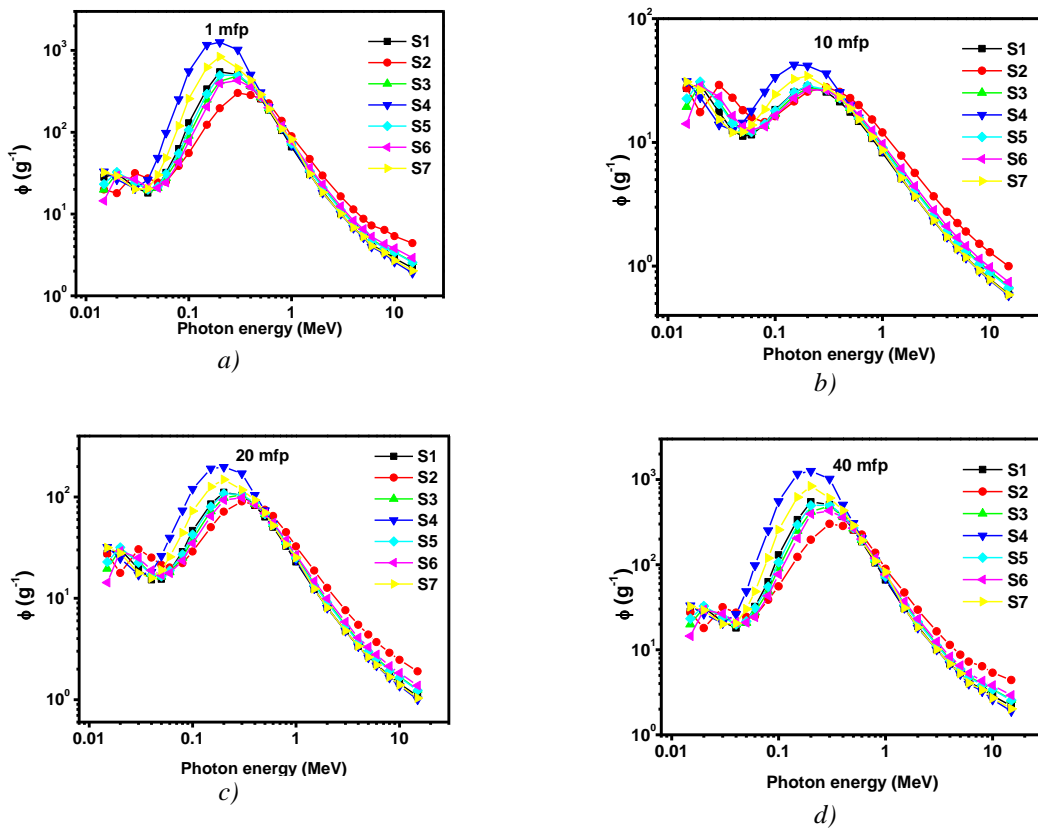


Fig. 5. The variation of specific fraction of absorbed energy ( $\Phi$ ) with incident photon for all bioactive glasses at  $r = 1$  mm at a) 1 mfp; b) 10 mfp; c) 20 mfp; d) 40 mfp.



The variations of specific fraction of absorbed energy ( $\Phi$ ) with penetration depths at 0.015, 0.15, 1.5 and 15 MeV are shown in Figs. (6-8). The specific fraction of absorbed energy increases with penetration depth. With increase in penetration depth, thickness of the interacting material increases, this results in increase of scattering events in target medium. Hence it results in large specific fraction of absorbed energy ( $\Phi$ ) values. To investigate the composition dependence of specific fraction of absorbed energy, we have studied the variation of specific fraction of absorbed energy ( $\Phi$ ) with  $Z_{\text{eff}}$ . Figs. 9 shows variation of specific fraction of absorbed energy ( $\Phi$ ) with  $Z_{\text{eff}}$  at 1mfp and 10 mfp, for some randomly selected values of incident photon energies. Specific fraction of absorbed energy ( $\Phi$ ) values decreases with increase of  $Z_{\text{eff}}$ . This confirms the fact that the chemical composition of different types of bio active gases affects their energy absorption properties of the medium.

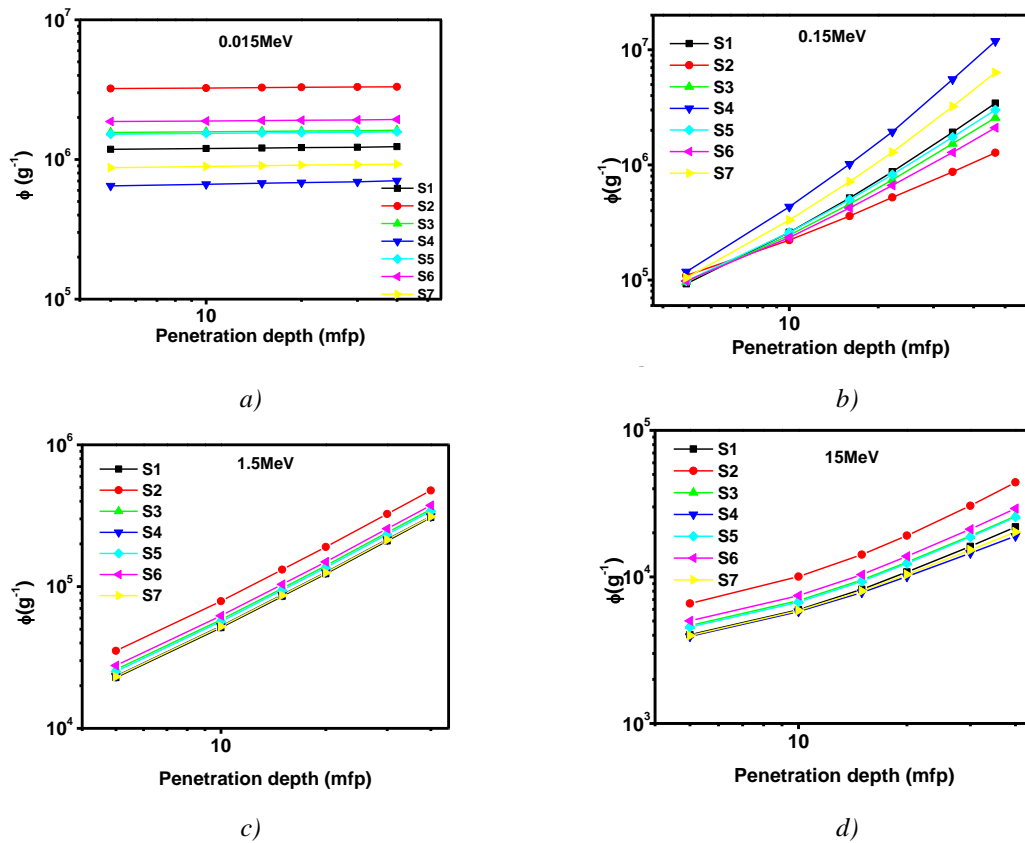


Fig. 6. The variation of specific fraction of absorbed energy ( $\Phi$ ) with penetration depth for all bioactive glasses at  $r = 0.01\text{mm}$  at a) 0.015 MeV; b) 0.15 MeV; c) 1.5 MeV; d) 15 MeV.

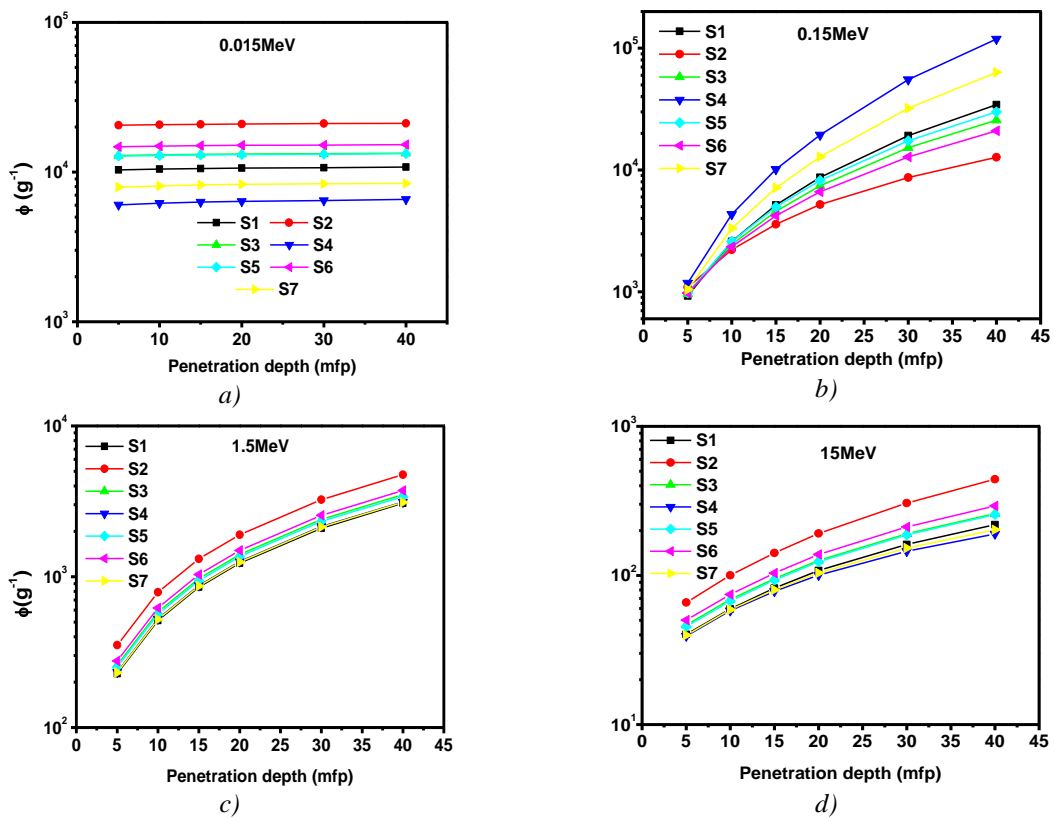


Fig. 7. The variation of specific fraction of absorbed energy ( $\Phi$ ) with penetration depth for all bioactive glasses at  $r = 0.1 \text{ mm}$  at a) 0.015 MeV; b) 0.15 MeV; c) 1.5 MeV; d) 15 MeV.

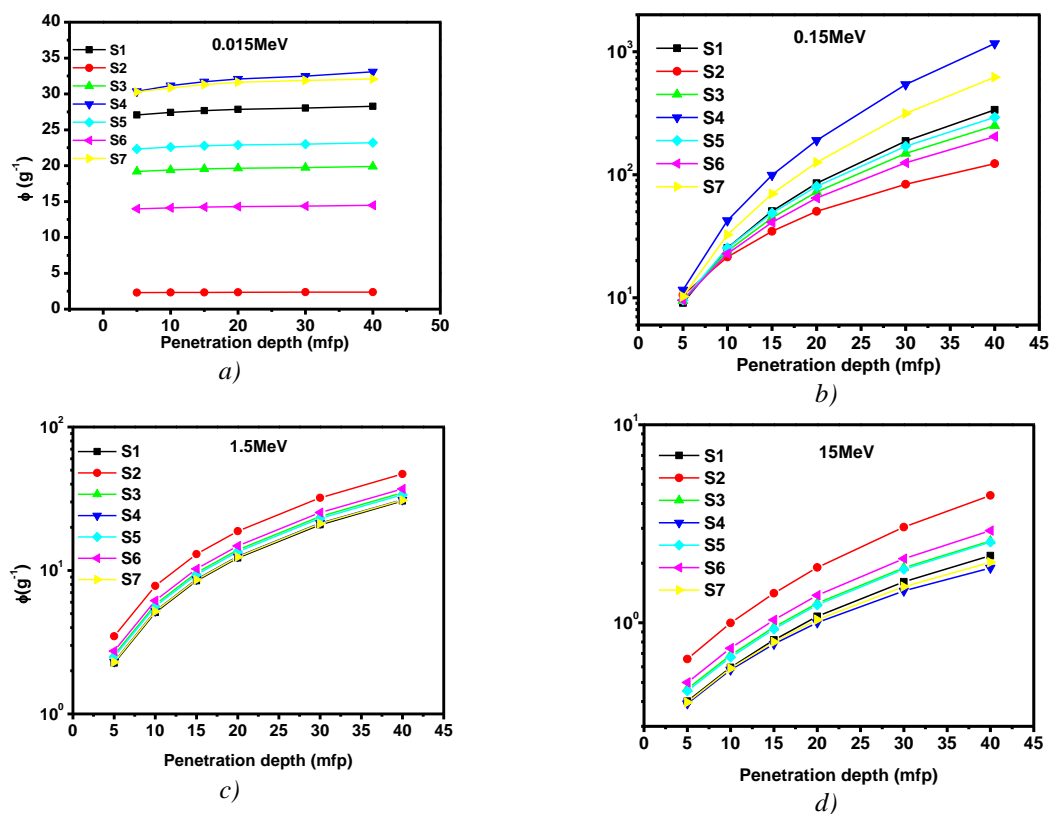


Fig. 8 The variation of specific fraction of absorbed energy ( $\Phi$ ) with penetration depth for all bioactive glasses at  $r = 1 \text{ mm}$  at a) 0.015 MeV; b) 0.15 MeV; c) 1.5 MeV; d) 15 MeV.

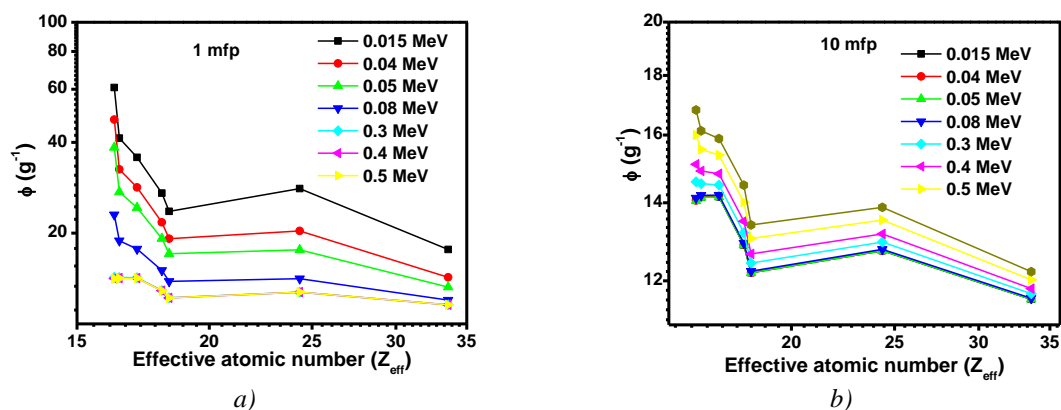


Fig. 9 The variation of specific fraction of absorbed energy ( $\Phi$ ) with effective atomic number for all bioactive glasses at  $r = 1\text{ mfp}$ , a)  $1\text{ mfp}$ ; b)  $10\text{ mfp}$ .

#### 4. Conclusions

In the present study, we studied effective atomic number, energy-absorption buildup factor and specific absorbed fractions of energy for different bioactive glasses. The results show that the energy-absorption buildup factor and specific absorbed fractions of energy are highest in medium energy range while minimum in both low and high photon energies. The effective atomic number for S2 was found the largest whereas; the energy-absorption buildup factor and specific absorbed fraction for S4 were found the largest. This study could be very useful in selection of a suitable type of bioactive glasses which in turn are able to resist possible radiation damages at human body.

#### References

- [1] S. M. Salman, S. N. Salman, H. A. Abo-Mosallam, *Ceramics International* **38**, 55 (2012).
- [2] L. L. Hench, *J. Mater. Sci.: Mater. Med.* **17**, 967 (2006).
- [3] S. Seuss, M. Heinloth, A. R. Boccaccini, *Surface & Coatings Technology* **301**, 100 (2016).
- [4] N. Huebsch, D. J. Moone, *Nature* **462**, 426 (2009).
- [5] N. Chanthima, J. Kaewkhao, *Annals of Nuclear Energy* **55**, 23 (2013).
- [6] S. J. Hosseinimehr, *Drug Discovery Today* **12**, (2007) 794-805.
- [7] G. S. Sidhu, P. S. Singh, G. S. Mudahar, *Journal of Radiological Protection* **20**, 53 (2000)
- [8] Y. Harima, Y. Sakamoto, S. Tanaka, M. Kawai, *Nucl. Sci. Eng.* **94**, 24 (1986).
- [9] M. I. Sayyed, H. Elhouichet, *Radit. Phys. Chem.* 335 (2017).
- [10] Mengge Dong, Xiangxin Xue, Ashok Kumar, He Yang, M. I. Sayyed, Shan Liu, Erjun Bu, *Journal of Hazardous Materials* **344**, 602 (2018).
- [11] M. I. Sayyed, G. Lakshminarayana, M. G. Dong, M. Çelikkilek Ersundu, A. E. Ersundu, I. V. Kityk, *Radiation Physics and Chemistry* **145**, 26 (2018).
- [12] V. P. Singh, N. M. Badiger, *J. Radioanal. Nucl. Chem.* **303**, 1983 (2015).
- [13] M. I. Sayyed, *Journal of Alloys and Compounds* **688**, 111 (2016)
- [14] L. Gerward, N. Guilbert, K. B. Jensen, H. Levring, *Radiation Physics and Chemistry* **71**, 653 (2004).
- [15] G. Lakshminarayana, Ashok Kumar, M. G. Dong, M. I. Sayyed, Nguyen Viet Long, M. A. Mahdi, *Journal of Non-Crystalline Solids* **481**, 65 (2018).
- [16] R. El-Mallawany, M. I. Sayyed, M. G. Dong, *Journal of Non-Crystalline Solids* **474**, 16 (2017).
- [17] S. R. Manohara, S. M. Hanagodimath, *Nuclear Instruments and Methods in Physics Research B* **264**, 9 (2007).
- [18] ANSI/ANS-6.4.3. 1991. *Gamma Ray Attenuation Coefficient and Buildup Factors for Engineering Materials* American Nuclear Society, La Grange Park, IL.

- [19] Y. Harima, Radiat.Phys. Chem. **41**, 631 (1993).
- [20] H. C. Manjunatha, B. Rudraswamy, Radiation Measurements **47**, 364 (2012)
- [21] H. C. Manjunatha, B. Rudraswamy, Annals of nuclear energy, **38**, 2271 (2011).